Water-Based Amorphous Carbon Nanotubes Filled Polymer Nanocomposites

Xiaoming Yang,[1,2] Liang Li,[2,3] Songmin Shang,[2] Xiao-ming Tao[2]

[1]*College of Chemistry, Chemical Engineering and Materials Sciences, Soochow University, Suzhou 215123, China*
[2]*Institute of Textiles and Clothing, The Hong Kong Polytechnic University, Hong Kong, China*
[3]*Key Laboratory for Green Chemical Process of Ministry of Education, School of Materials Science and Engineering, Wuhan Institute of Technology, Wuhan 430073, China*

Received 5 October 2010; accepted 28 December 2010
DOI 10.1002/app.34072
Published online 13 June 2011 in Wiley Online Library (wileyonlinelibrary.com).

ABSTRACT: A novel method of making water-based amorphous carbon nanotubes (ACNTs) for advanced polymer nanocomposites is presented. In this approach, sodium dodecyl sulfate (SDS) is introduced onto the amorphous carbon nanotubes to improve the solubility in water and the dispersion in polyvinyl alcohol [PVA] matrix. As a result, the addition of 0.6 wt % ACNTs in the polymer resulted in the significant improvement (167.5 and 175.8%) in the tensile strength and modulus of the polymer, respectively. The improved mechanical property could be ascribed to the load transfer to the nanotubes in the composites. © 2011 Wiley Periodicals, Inc. J Appl Polym Sci 122: 1986–1992, 2011

Key words: composites; nanocomposites; mechanical properties

INTRODUCTION

Since carbon nanotubes (CNTs) were reported, the unique structures and extraordinary properties of CNTs have attracted a tremendous amount of interest in both fundamental and technological development.[1] They have also attracted great attention as advanced reinforcing fillers for high-strength, lightweight, and functional polymer nanocomposites due to their unique structural, mechanical, electrical, and thermal properties.[2–4] The use of these nanotubes as a filler offers an important advantage over conventional fillers.[5–7] The extremely high aspect ratio of the nanotubes implies that low loading of the nanotubes is sufficient to change a desired property without sacrificing other inherent properties of the polymer.[8,9]

However, such high-performance carbon-nanotube-based composites face a number of practical challenges before their true potential performance can be implemented. First, a homogenous dispersion of carbon nanotubes in their host polymer matrix must be achieved. Indeed, the intrinsic van der Waals attraction of nanotubes toward each other easily leads to entangled agglomerates, which results in the insolubility of carbon nanotubes in most organic and aqueous solvents. Such agglomerates lower the effectiveness of nanotubes for reinforcement. The functionalization of CNTs is an effective way to prevent them from aggregation allowing for better dispersion and to stabilize the CNTs within a polymer matrix.[10]

A number of research groups have used chemically functionalized nanotubes as polymer–composite reinforcement. For example, Geng et al. have obtained a 145% tensile–modulus improvement with only 1 wt % fluorinated Single-walled Carbon Nanotubes (SWNTs) in a poly(ethylene oxide) matrix.[11] In another recent study, the tensile modulus was increased by 21% using 10 wt % SWNTs in polybutoxide poly(*p*-phenylene benzobisoxazole) fibers.[12] Moreover, a 27% tensile-modulus improvement was obtained through the addition of 1 wt % of SWNTs into epoxy reins.[13] However, these modifications may destroy the integrity of the nanotubes to some extent and the process is complex.

Correspondence to: X. Yang (yangxiaoming@suda.edu.cn) and S. Shang (tcshang@inet.polyu.edu.hk).

Contract grant sponsor: Educational Bureau of Jiangsu Province; contract grant number: 10KJB430013.
Contract grant sponsor: Educational Bureau of Hubei Province; contract grant number: Q20091508.
Contract grant sponsor: Scientific Research Foundation for Returned Overseas Chinese Scholars of MOE; contract grant number: ([2009]1341).
Contract grant sponsor: Scientific Research Key Project of MOE; contract grant number: 209081.
Contract grant sponsor: National Natural Science Foundation of China; contract grant number: 20904044.
Contract grant sponsor: The Hong Kong Polytechnic University.
Contract grant sponsor: Key Project in Science and Technology Innovation Cultivation Program of Soochow University

At present, although nanocomposites employing carbon based reinforcement materials are dominated by carbon nanotubes, the intrinsic bundling of carbon nanotubes, their intrinsic impurities from catalysts, and their high cost have still been hampering their application. New materials such as graphite oxide[14,15] and graphene have recently attracted tremendous attention.[16,17] Chen et al. have prepared poly(vinyl alcohol) (PVA) nanocomposites with graphite oxide using simple water solution processing method, 76% increase in tensile strength and 62% improvement of modulus are achieved by addition of only 0.7 wt % of graphite oxide.[15] Other types of advanced reinforcing fillers are attracting a tremendous amount of interest.

In our previous study, we synthesize the carbon nanotubes via the pyrolysis of the polypyrrole (PPy) nanotubes at 900°C in nitrogen atmosphere.[18,19] This synthesis method of the carbon nanotubes is simple and would be an easy way to produce more nanotubes on a large scale. Interestingly, these carbon nanotubes were found to be mostly amorphous in structure. In this study, these amorphous carbon nanotubes (ACNTs) were studied as a new filler in polymer matrix. Currently, various methods are used to incorporate carbon nanotubes into a polymer matrix, e.g., solution casting, melt mixing, electron spinning, and *in situ* polymerization.[20–25] Among these methods, solution casting is a common and simple method, which is particularly useful for common polymers. In this article, the ACNTs-poly (vinyl alcohol) (PVA) nanocomposites were chosen to understand the properties of the nancomposites. They were characterized in terms of the mechanical and thermal properties. The composites exhibit good nanotube dispersion and load transfer from polymer matrix to the carbon nanotubes.

EXPERIMENT

Materials

sodium dodecyl sulfate (SDS), polypyrrole (Ppy), PVA (99+% hydrolyzed, $M_w \sim$ 89,000–98,000) were purchased from Aldrich. Other reagents were of analytical grade and used without further purification.

Synthesis of hybrid materials

PPy nanotubes were produced according to the previous article.[18] ACNTs were fabricated by carbonization of PPy nanotubes in a quartz tubular furnace under nitrogen atmosphere. The sample was gradually heated up to 900°C at a heating rate of 3°C min^{-1}, held 900°C for 5 h and then cooled to room temperature.[19]

The ACNTs aqueous dispersion assisted by sodium dodecyl sulfate (SDS) was prepared according to the previously published procedure. ACNTs were dispersed in SDS aqueous (1 wt %) solution followed by homogenization, ultrasonication. The residual SDS was removed by repeated centrifugation and ultrasonication. SDS/ACNTs aqueous dispersion was obtained.

PVA was dissolved in distilled water at 90°C (to give 5 wt % solutions) and subsequently cooled to room temperature.

An appropriate amount of SDS/ACNTs aqueous dispersion was mixed with PVA solution at room temperature to give the desired 0.3, 0.6, 0.9, and 1.5 wt % ACNTs concentration with respect to the PVA weight. The mixture was mildly sonicated for 1 h at room temperature and stirred for about 24 h. The PVA/SDS/ACNTs dispersions were poured into Telfon Petri dished and kept in vacuum at 40°C for film formation until the weight reached an equilibrium value. The thickness of the resulting film was about 0.05 mm.

Characterization

The glass transition and crystallization behaviors were investigated by differential scanning calorimetry (DSC) using a Perking Elmer Pyris. The experiments were carried out in nitrogen atmosphere using about 5 mg sample sealed in aluminum pans. The samples were heated from room temperature to 240°C, maintained at this temperature for 5 min, then cooled to room temperature and heated again to 240°C. The heating and cooling rate were 10°C min^{-1} in all cases. The glass transition temperatures and melting enthalpy are taken from the second heating run in the calorimetric curves.

Thermogravimetric analysis (TGA) was performed on a Netzch STA 449C instrument at a heating rate of 10°C min^{-1} in an air atmosphere.

Scanning electron microscopy (SEM, JEOL Model JSM-6490) was used to observe the cross sections of the PVA/SDS/ACNTs nanocomposite films. The cross sections were coated with gold before analysis.

Raman spectra was recorded in the range of 0–3500 cm^{-1} at ambient temperature with a labRAM HR 800 (France, Jobin Yvon) using 532 nm laser as the excitation source.

The mechanical properties of PVA/SDS/ACNTs films were measured on a universal tensile testing machine (Instron 4411). Before testing, vacuum oven dried samples were conditioned in the laboratory environment (20°C with 60% relative humidity) for 24 h before testing, as PVA exhibit a high degree of moisture sensitivity. The specimen dimension was 60 mm in length, 10 mm in width, and 0.05 mm in

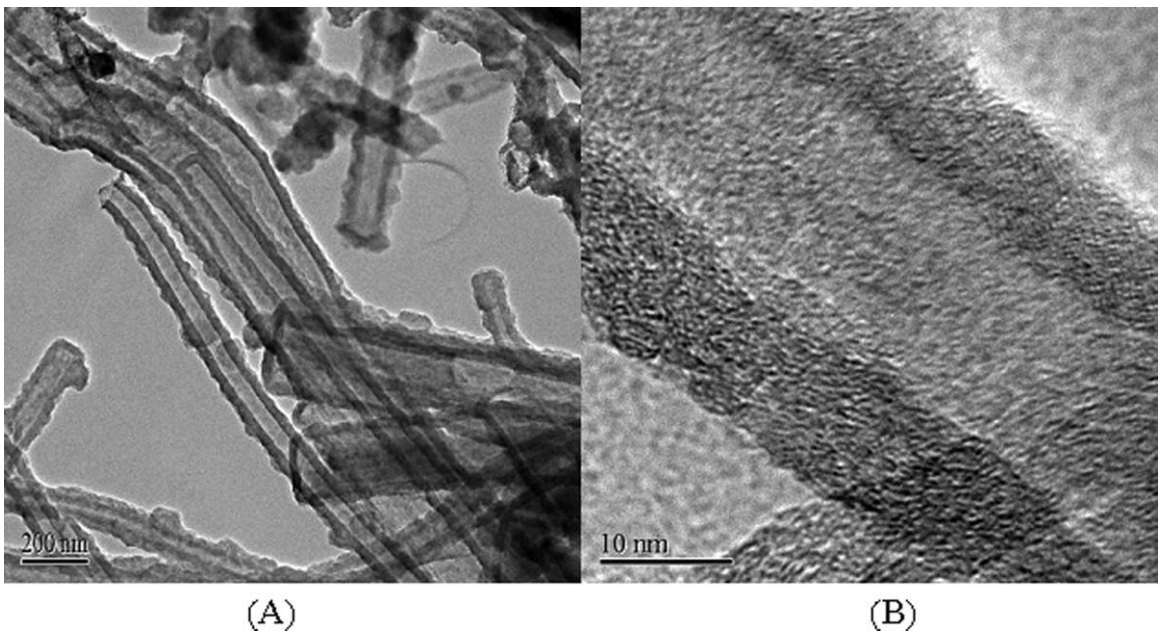

Figure 1 (A) The TEM image of ACNTs; (B) the HRTEM image of ACNTs.

thickness. The extension rate was 5 mm min^{-1} and the load cell was 250*N* with a gauge length of 40 mm. The data on modulus, tensile stress, and strain at rupture were the averages of five strips of the sample. All failure occurred at the middle region of the testing strips.

RESULTS AND DISCUSSION

Figure 1 shows the TEM image of amorphous carbon nanotubes prepared by pyrolysis of the polypyrrole nanotubes. It was evident from Figure 1(A) that the tubular structures were obtained after pyrolysis. The wall thickness of the carbon nanotube is around 10–25 nm. The HRTEM image of the ACNTs shows that these carbon nanotubes are mostly amorphous in structure.

From Figure 2(A) it can be observed that the ACNTs can be dispersed in aqueous medium more easily than the commercials CNTs. The possible reason is that CNTs are tightly bundled as a result of strong van der Waals interactions while ACNTs are not tightly bundled [Fig. 1(A)]. Surfactants (such as SDS, polysaccharide) were always used to disperse CNTs in aqueous solutions. In some cases, the dispersant is able to disperse but not to exfoliate the CNTs. So CNTs may aggregate again during the composite forming process.

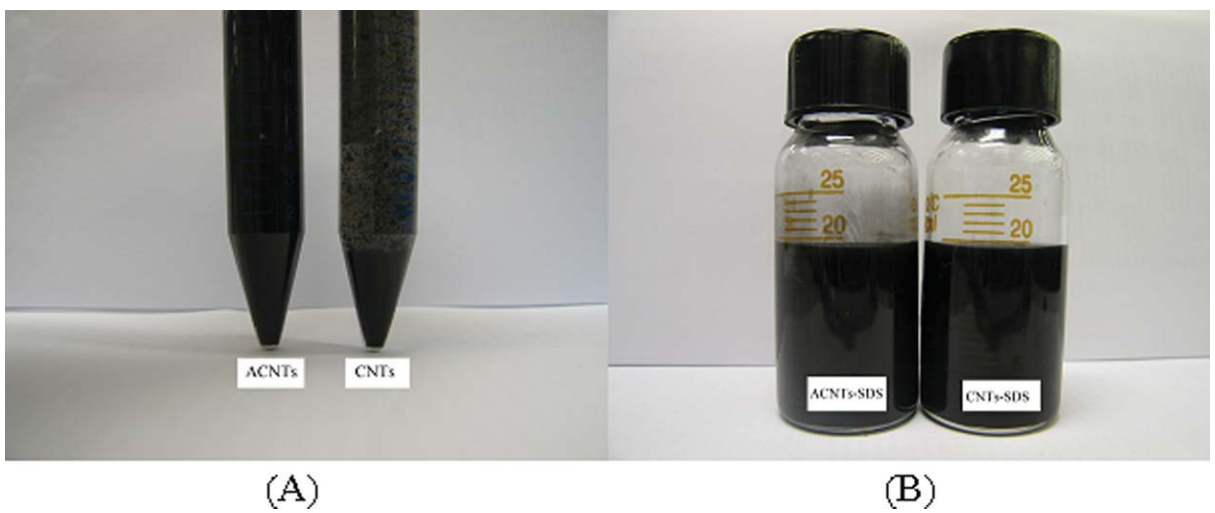

Figure 2 (A) The photograph of ACNTs and CNTs dispersed in aqueous solutions, respectively; (B) the photograph of SDS modified ACNTs and CNTs dispersed in aqueous solutions. [Color figure can be viewed in the online issue, which is available at wileyonlinelibrary.com.]

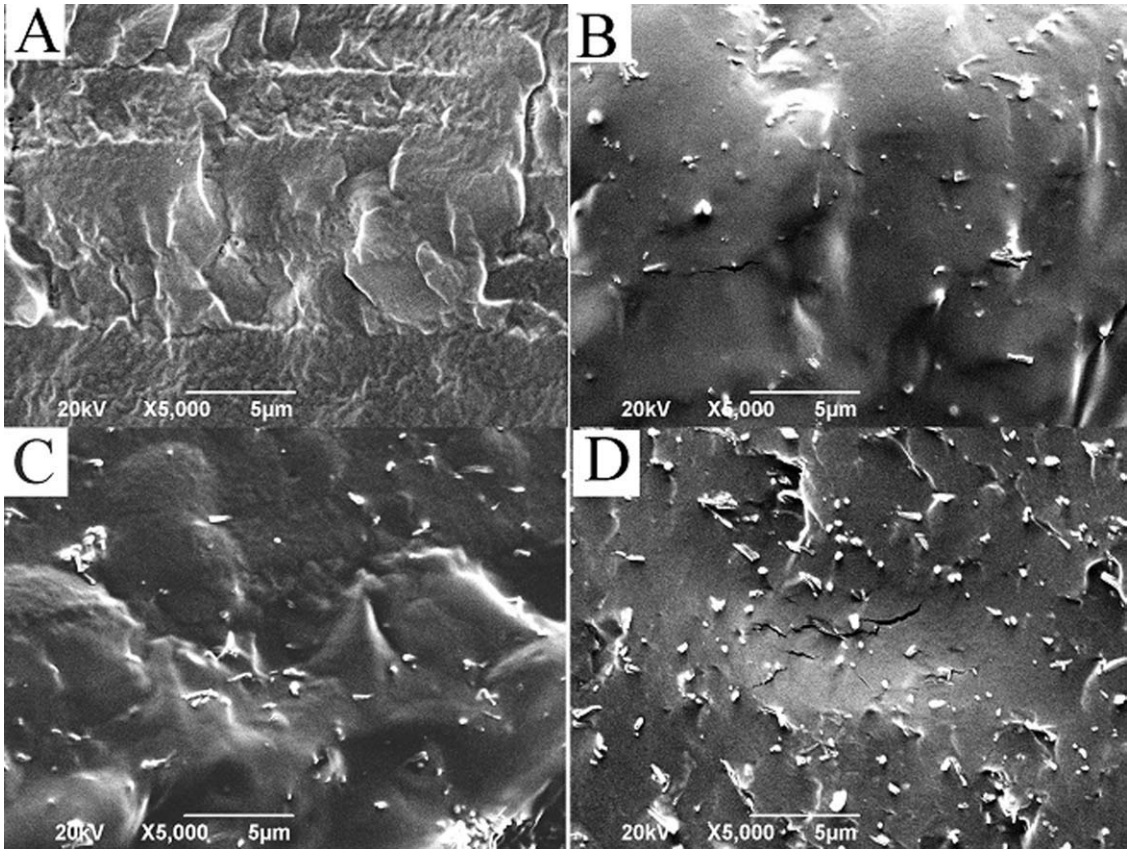

Figure 3 SEM images of the cross section of PVA/SDS/ACNTs nanocomposites with different ACNTs contents. A: 0; B: 0.6 wt %; C: 0.9 wt %; D: 1.5 wt %.

In this study, to obtain a homogeneous dispersion of the individual ACNTs throughout a water-soluble polymer matrix, and simultaneously to achieve and enhanced interfacial adhesion between the ACNTs and polymer matrix, sodium dodecyl sulfate (SDS) was chosen to modification the surface of ACNTs. From Figure 2(B), it can be seen that homogeneous dispersion of SDS modified ACNTs can be easily obtained. Finally a homogenous and uniform composite film (PVA/SDS/ACNTs) can be observed.

The cross section of the nanocomposites after fractured in liquid nitrogen was investigated by SEM to verify the dispersion and the possible reinforcing mechanism of the nanocomposites. As shown in Figure 3, the pure PVA is characterized with surface with no bright dots. In contrast, The SEM images of the fracture surface of the PVA/SDS/ACNTs nanocomposite films clearly show well-dispersed bright dots, which are the ends of the broken ACNTs. It could be concluded that SDS functionalized ACNTs displayed good dispersion ability in the PVA matrix. It can be predicted from these results that the existing strong interfacial adhesion is responsible for the vigorous enhancement of the mechanical properties of the nanocomposites as discussed in the next section.

Raman spectroscopy is a useful nondestructive tool to investigate the structure changes of carbonaceous materials. As shown in Figure 4, The SDS/ACNTs has two characteristic peaks at 1337 and 1572 cm^{-1}, corresponding to the D-band (C—C, the disordered graphite structure) and G-band (C=C,

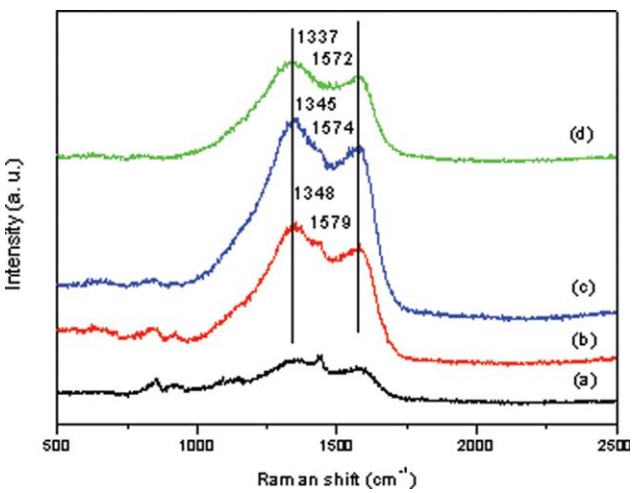

Figure 4 Raman spectra of (a) PVA, (b) PVA/SDS/ACNTs (0.6 wt %), (c) PVA/SDS/ACNTs (0.3 wt %) and (d) SDS/ACNTs. [Color figure can be viewed in the online issue, which is available at wileyonlinelibrary.com.]

TABLE I
Raman I_D/I_G Intensity Ratios and D- and G-Bands Shifts of SDS/ACNTs and PVA/SDS/ACNTs Composites

	SDS/ ACNTs	PVA/SDS/ ACNTs (0.3 wt%)	PVA/SDS/ ACNTs (0.6 wt%)
I_D/I_G	1.16	1.17	1.20
D-band (cm^{-1})	1337	1345	1348
G-band (cm^{-1})	1572	1574	1579

sp2-hybridized carbon), respectively.[26] The ratio of D- to G-band intensity (I_D/I_G) could be used to indicate the structure changes of carbon nanotubes.[27] As listed in Table I, I_D/I_G of ACNTs is 1.16, while I_D/I_G of the PVD/SDS/ACNTs nanocomposite increases to 1.20. Moreover, the frequencies of the D-band and G-band of PVA/SDS/ACNTs nanocomposite are shifted upward by 11 and 7 cm^{-1}, respectively. The higher I_D/I_G ratio and the upshift of D- and G-bands were attributed to charge transfer between carbon nanotubes and matrix polymer[28,29] or the increase in the numbers of the sp3-hybridized sidewall carbons caused by functionalization and adherence of polymers on carbon nanotubes.[30–32] Thus, this result is a qualitative evidence to imply the interaction between ACNTs to PVA matrix.

Mechanical behavior of PVA-ACNTs nanocomposite

Tensile testing was performed to evaluate the effect of nanotubes on the mechanical properties of the nanocomposites.

Figure 5 shows the typical stress–strain behaviors of PVA/ACNTs films. In this situation, SDS was not used to disperse the ACNTs in polymer matrix. Compared with the PVA, tensile yield strength of PVA/ACNTs, containing only 0.6 wt % increased by

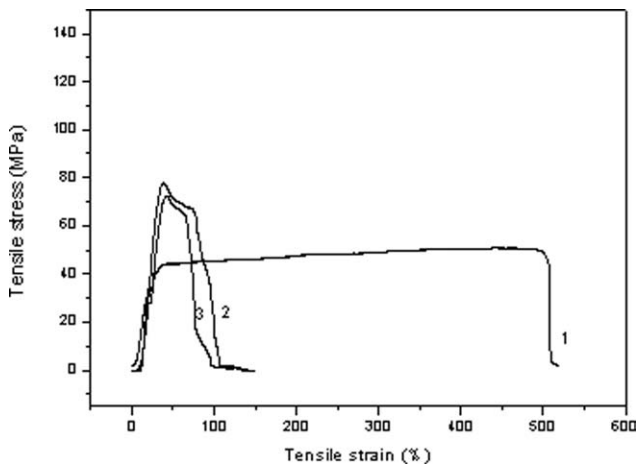

Figure 5 Typical stress-strain behaviors for the PVA/ ACNTs films with different ACNTs, (1): 0; (2): 0.3 wt%; (3): 0.6 wt%.

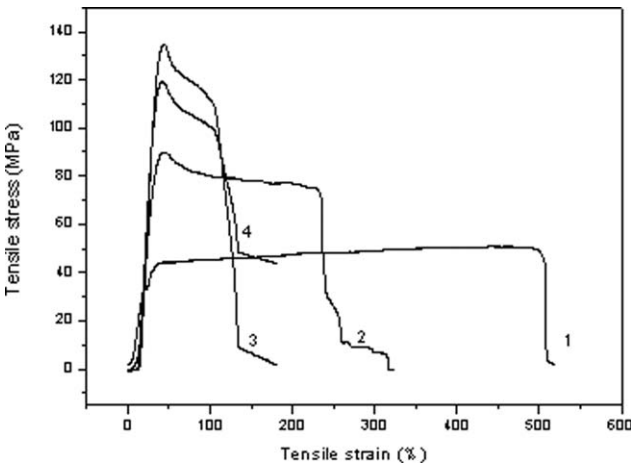

Figure 6 Typical stress-strain behaviors for the PVA/ SDS/ACNTs films with different ACNTs, (1): 0; (2): 0.3 wt%; (3): 0.6 wt%; (4): 0.9 wt%.

41.6% from 36 to 51 MPa, and the Young's modulus increases by 47.06% from 1.7 to 2.5 GPa.

The typical stress-strain curves for PVA and PVA/SDS/ACNTs films are given in Figure 6. Tensile strength of PVA/SDS/ACNTs is much higher than that of PVA film. The tensile strength and modulus were calculated from the stress–strain profiles. Compared to the PVA, tensile yield strength of PVA/SDS/ACNTs, containing only 0.6 wt % increased by 167.5% from 36 to 96.3 MPa, and the Young's modulus increases by 175.8% from 1.7 to 4.7 GPa (As shown in Table II). However, Increasing the ACNTs content up to 0.9% did not increase the tensile yield strength and Young's modulus of the composites. The possible reason is the aggregation of the ACNTs at higher concentration.[33–35]

The results indicate that the reinforcing effect of the ACNTs is pronounced. Several conclusions may be drawn from the results obtained so far. First, from the observation by SEM images (Fig. 3), it was clearly known that a good dispersion of ACNTs was achieved throughout the PVA matrix, which led to a significant increase in the tensile strength of the nanocomposite. Second, the incorporation of the SDS

TABLE II
The Tensile Strength, Ultimate Elongation, Modulus of PVA/ ACNTs Nanocomposite with Different ACNTs Contents

Samples	Tensile strength (MPa)	Ultimate elongation (%)	Modulus (GPa)
Pure PVA	36	500	1.7
PVA/ACNTs 0.3 wt %	50	76	2.1
PVA/ACNTs 0.6 wt %	51	63	2.5
PVA/SDS/ACNTs 0.3 wt %	90	227	3.3
PVA/SDS/ACNTs 0.6 wt %	96.3	110	4.7
PVA/SDS/ACNTs 0.9 wt %	134	103	4.6

TABLE III
***Tg* of PVA/SDS/ACNTs Nanocomposite**

	PVA	PVA/SDS/ ACNTs (0.3 wt %)	PVA/SDS/ ACNTs (0.6 wt %)	PVA/SDS/ ACNTs (0.9 wt %)
T_g (°C)	76.7	70.0	71.0	71.8

functionalized ACNTs into the polymer matrix created some interactions between ACNTs and polymer chains, thus being favorable for stress transfer to ACNTs.

Crystallization of PVA/SDS/ACNTs

Differential scanning calorimetry (DSC) was used to compare the glass-transition temperature (T_g) of pure PVA with that of the PVA/SDS/ACNTs nanocomposite as shown in Table III.

The T_g of PVA/SDS/ACNTs nanocomposite with 0.3 wt % ACNTs loading decreased from 76.7 to 70°C. The T_g decreased at low nanotube fractions to a constant value about 6–7°C lower than the T_g of pure PVA, and did not change further as the nanotube amount changed from 0.3 to 1.5 wt %. Many studies involving CNTs-polymer composites have shown an increase.[36,37] as well as broadening[37,38,24,25] in T_g.[26,27,39,40] It is interesting but difficult to explain the decrease in T_g in our samples. There was a small decrease in T_g with added ACNTs, attributed to surfactant plasticization.[41–43,28–30] In our case, the absorbed SDS on the surface of ACNTs may result in the decrease of T_g.

Since PVA is a semicrystalline polymer, its mechanical properties strongly depend on the degree of its crystallinity. DSC was used to measure the melting enthalpy of pure PVA and PVA/SDS/ACNTs nanocomposites. For pure PVA and nanocomposite samples, the melt curves are shown in Figure 7. The crystallinity (χ_c), calculated as follows:

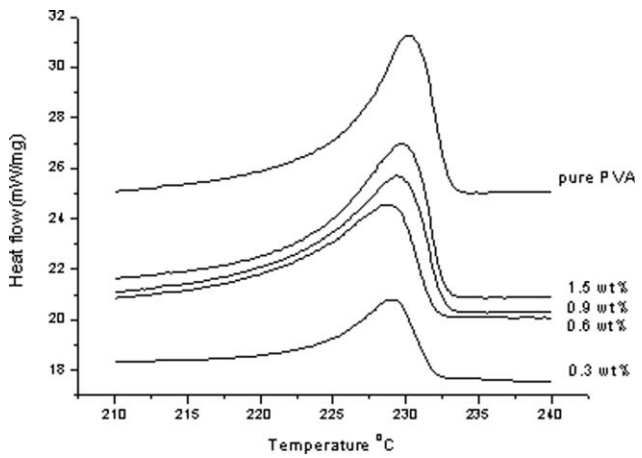

Figure 7 Melt curves of PVA/SDS/ACNTs nanocomposite with different ACNTs contents.

TABLE IV
The Crystallinity ((c) of PVA/SDS/ACNTs Nanocomposite with Different ACNTs Contents

Samples	ΔH_m (J g^{-1})	χ_c
Pure PVA	61.4	44.3
PVA-ACNTs 0.3 wt %	45.6	32.9
PVA-ACNTs 0.6 wt %	46.4	33.5
PVA-ACNTs 0.9 wt %	43.2	31.2

$$\chi_c = \frac{\Delta H_m}{\Delta H_0}$$

where ΔH_m is the measured melting enthalpy and is the enthalpy of pure PVA crystal (138.6 J g^{-1}).[44,45] The results are shown in Table IV.

As shown in Table IV, PVA crystallinity in PVA/SDS/ACNTs film containing 0.3 wt % is 25.7% lower compared with that of the pure PVA film. Therefore the increased modulus and strength in the nanotubes containing film is not attributed to changes in crystallinity. The significantly increased strength and modulus of the PVA-ACNTs nanocomposites can be attributed to the fillers. Similar results have been demonstrated for CNTs-based nanocomposites.[46,47]

Thermal stability of PVA/SDS/ACNTs nanocomposite

To investigate the thermal stability of the PVA/SDS/ACNTs nanocomposites, thermal gravimetric analysis (TGA) measurements were carried out, and the results are shown in Figure 8. In this study, the criterion for thermal stability was taken as the decomposition temperature. The decomposition of pure PVA occurred at 253°C. Compared to the pure PVA, the PVA/SDS/ACNTs films showed the delayed decomposition. The decomposition temperature for the nanocomposite

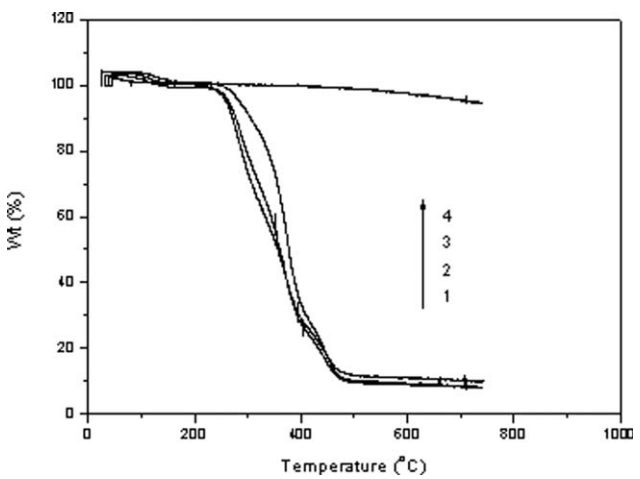

Figure 8 TGA curves of PVA/SDS/ACNTs with different of ACNTs content, (1) 0; (2): 0.9 wt%; (3): 1.5 wt%; (4) 100 wt%.

with ACNTs contents of 0.9 and 1.5 wt % increased by 5 and 25°C, respectively. So, the thermal stability of PVA was improved by adding ACNTs. This is because polymer chains near the ACNTs may degrade more slowly; another reason for the increased thermal stability of the polymer is due to the effect of higher thermal conductivity of ACNTs, which may facilitate heat dissipation within the polymer composite.[9] In addition, dispersed nanotubes might hinder the flux of decomposition products and hence delay decomposition. It is important to point out that the higher extent of interaction between the ACNTs and the PVA matrix could be responsible for the higher thermal stability of the nanocomposite.

CONCLUSIONS

We have successfully prepared PVA/SDS/ACNTs nanocomposites by simple water solution processing method. Though the addition of ACNTs decreases the crystallinity of PVA, the film of the PVA/graphene nanocomposite is strong. The modulus and tensile strength of PVA/SDS/ACNTs nanocomposite containing only 0.6 wt % ACNTs were increased by 167.5% from 36 to 96.3 MPa, and the Young's modulus were increased by 175.8% from 1.7 to 4.7 GPa. And the thermal stability improved to some extent. On the basis of the results, the influence in the thermal and mechanical properties of the nanocomposites can be ascribed mainly to the homogeneous dispersion of ACNTs in PVA matrix and the interactions between both components. It demonstrates that ACNTs can be utilized effectively as fillers within the polymer matrix for the large-scale potential applications for polymer/ACNTs nanocomposites.

References

1. Iijima, S. Nature 1991, 354, 56.
2. Baughman, R. H.; Zakhidov, A. A.; de Heer, W. A. Science 2002, 297, 787.
3. Xie, X. L.; Mai, Y. W.; Zhou, X. P. Mater Sci Eng R Rep 2005, 49, 89.
4. Treacy, M. M.; Ebessen, T. W.; Gibson, J. M. Nature 1996, 381, 678.
5. Abdalla, M.; Dean, D.; Theodore, M.; Fielding, J.; Nyairo, E; Price, G. Polymer 2010, 51, 1614.
6. Zeng, C.; Hossieny, N.; Zhang, C.; Wang, B. Polymer 2010, 51, 655.
7. Foster, R. J.; Hine, P. J.; Ward, I. M. Polymer 2009, 50, 4018.
8. Salvetat, J. P.; Briggs, G. A. D.; Bonard, J. M.; Bacsa, R. R.; Kulik, A. J.; Stockli, T.; Burnham, N. A.; Forro, L. Phys ReV Lett 1999, 82, 944.
9. Moniruzzaman, M.; Winey, K. I. Macromolecules 2006, 39, 5194.
10. Sahoo, N. G.; Cheng, H. K. F.; Li, L.; Chan, S. H.; Judeh, Z.; Zhao, J. H. Adv Funct Mater 2009, 19, 3962.
11. Geng, H. Z.; Rosen, R.; Zheng, B.; Shimoda, H.; Fleming, L.; Liu, J.; Zhou, O. Adv Mater 2002, 14, 1387.
12. Kumar, S.; Dang, T. D.; Arnold, F. E.; Bhattacharyya, A. R.; Min, B. G.; Zhang, X. F.; Vaia, R. A.; Park, C.; Adams, W. W.; Hauge, R. H.; Smalley, R. E.; Ramesh, S.; Willis, P. A. Macromolecules 2002, 35, 9039.
13. Zhu, J.; Kim, J. D.; Peng, H. Q.; Margrave, J. L.; Khabashesku, V. N.; Barrera, E. V. INano Lett 2003, 3, 1107.
14. Jeong, H. K.; Jin, M. H.; An, K. H.; Lee, Y. H. J Phys Chem C 2009, 113, 13060.
15. Liang, J. J.; Huang, Y.; Zhang, L.; Wang, Y.; Ma, Y. F.; Guo, T. Y.; Chen, Y. S. Adv Funct Mater 2009, 19, 2297.
16. Rafiee, M. A.; Rafiee, J.; Srivastava, I.; Wang, Z.; Song, H. H.; Yu, Z. Z.; Koratkar, N. Small 2010, 6, 179.
17. Stankovich. S.; Dikin, D. A.; Dommett, G. H. B.; Kohlhaas, K. M.; Zimney, E. J.; Stach, E. A.; Piner, R. D.; Nguyen, S. T.; Ruoff, R. S. Nature 2006, 442, 282.
18. Yang, X. M.; Zhu, Z. X.; Dai, T. Y.; Lu, Y. Macromol Rapid Commun 2005, 26, 1736.
19. Shang, S. M.; Yang, X. M.; Tao, X. M. Polymer 2009, 50, 2815.
20. Sahoo, N. G.; Jung, Y. C.; Yoo, H. J.; Cho, J. W. Macromol Chem Phys 2006, 207, 1773.
21. Liu, T. X.; Phang, I. Y.; Shen, L.; Chow, S. Y.; Zhang, W. D. Macromolecules 2004, 37, 7214.
22. Sen, R.; Zhao, B.; Perea, D.; Itkis, M. E.; Hu, H.; Love, J.; Bekyarova, E.; Haddon, R. C. Nano Lett 2004, 4, 459.
23. Hou, H. Q.; Ge, J. J.; Zeng, J.; Li, Q.; Reneker, D. H.; Greiner, A.; Cheng, S. Z. D. Chem Mater 2005, 17, 967.
24. So, H. H.; Cho, J. W.; Sahoo, N. G. Eur Polym Mater 2007, 43, 3750.
25. Yoo, H. J.; Jung, Y. C.; Sahoo, N. G.; Cho, J. W. J Macromol Sci Part B Phys 2006, 45, 441.
26. Price, B. K.; Hudson, J. L.; Tour, J. M. J Am Chem Soc 2005, 127, 14867.
27. Alvarez, L.; Righi, A.; Guillard, T.; Rols, S.; Anglaret, E.; Laplaze, D.; Sauvajol, J. L. Chem Phys Lett 2000, 316, 186.
28. Wise, K. E.; Park, C.; Siochi, E. J.; Harrison, J. S. Chem Phys Lett 2004, 391, 207.
29. Xu, X.; Uddin, A. J.; Aoki, K.; Gotoh, Y.; Saito, T.; Yumur, M. Carbon 2010, 48, 1977.
30. Zhang, L.; Kiny, V. U.; Peng, H.; Zhu, J.; Lobo, R. F. M.; Margrave, J. L.; Khabashesku, V. N. Chem Mater 2004, 16, 2055.
31. Zhao, Q.; Wagner, H. D. Philos Trans R Soc London Ser A 2004, 362, 2407.
32. Mahanandia, P.; Schneider, J. J.; Khaneft, M.; Stuhn, B.; Peixotob, T. P.; Drossel, B. Phys Chem Chem Phys 2010, 12, 4407.
33. Xu, X. Z.; Uddin, A. J.; Aoki, K.; Gotoh, Y.; Saito, T. Carbon 2010, 48, 1977.
34. Lee, B. S.; Yu, W. R. Macromol Res 2010, 18, 162.
35. Bin, Y.; Kitanaka, M.; Zhu, D.; Matsuo, M. Macromolecules 2003, 36, 6213.
36. Yang, Y. K.; Xie, X. L.; Wu, J. G.; Mai, Y. W. J Polym Sci A Polym Chem 2006, 44, 3869.
37. Putz, K. W.; Mitchell, C. A.; Krishnamoorti, R.; Green, P. F. J Polym Sci B Polym Phys 2004, 42, 2286.
38. Miaudet, P.; Derre, A.; Maugey, M.; Zakri, C.; Piccione, P. M.; Inoubli, R.; Poulin, P. Science 2007, 318, 1294.
39. Jin, S. H.; Choi, D. K.; Lee, D. S. Colloid Surf A 2008, 313, 242.
40. Ha, M. L. P.; Grady, B. P.; Lolli, G.; Resasco, D. E.; Ford, W. T. Macromol Chem Phys 2007, 208, 446.
41. Xia, H. S.; Song, M. J Mater Chem 2006, 16, 1843.
42. Shieh, Y. T.; Liu, G. L. J Polym Sci B Polym Phys 2007, 45, 1870.
43. Grady, B. P.; Paul, A.; Peters, J. E.; Ford, W. T. Macromolecules 2009, 42, 6152.
44. Cerezo, F. T.; Preston, C. M. L.; Shanks, R. A. Macromol Mater Eng 2007, 292, 155.
45. Su, J. X.; Wang, Q.; Su, R.; Wang, K.; Zhang, Q.; Fu, Q. J Appl Polym Sci 2008, 107, 4070.
46. Liu, L. Q.; Barber, A. H.; Nuriel, S.; Wagner, H. D. Adv Funct Mater 2005, 15, 975.
47. Zhang, X. F.; Liu, T.; Sreekumar, T. V.; Kumar, S.; Moore, V. C.; Hauge, R. H. Nano Lett 2003, 3, 1285.